

See discussions, stats, and author profiles for this publication at: <https://www.researchgate.net/publication/50302868>

# Study on the Effects of Humic and Fulvic Acids on Quantum Dot Nanoparticles Using Capillary Electrophoresis with Laser-Induced Fluorescence Detection

ARTICLE *in* ENVIRONMENTAL SCIENCE & TECHNOLOGY · MARCH 2011

Impact Factor: 5.33 · DOI: 10.1021/es1031097 · Source: PubMed

---

CITATIONS

17

---

READS

14

4 AUTHORS, INCLUDING:



Luis A Colón

University at Buffalo, The State University of ...

81 PUBLICATIONS 2,284 CITATIONS

SEE PROFILE



Diana S Aga

University at Buffalo, The State University of ...

125 PUBLICATIONS 3,647 CITATIONS

SEE PROFILE

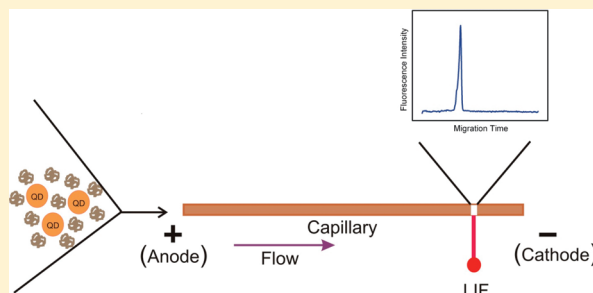
# Study on the Effects of Humic and Fulvic Acids on Quantum Dot Nanoparticles Using Capillary Electrophoresis with Laser-Induced Fluorescence Detection

Mary Dawn Celiz, Luis A. Colón,\* David F. Watson, and Diana S. Aga\*

Department of Chemistry, Natural Sciences Complex, University at Buffalo, The State University of New York, Buffalo, New York 14260-3000, United States

**S** Supporting Information

**ABSTRACT:** The increasing production and use of quantum dot (QD) nanoparticles have caused concerns on the possibility of contaminating the aquatic and terrestrial ecosystems with wastes that may contain QDs. Therefore, studies on the behavior of QDs upon interaction with components of the natural environment have become of interest. This study investigated the fluorescence and electrophoretic mobility of carboxylic or amine polyethylene glycol (PEG)-functionalized CdSe/ZnS QDs in the presence of two aquatic humic substances (HS), Suwannee River humic and fulvic acids, using capillary electrophoresis with laser-induced fluorescence detection. Results showed initial enhancement in fluorescence of QDs at the onset of the interaction with HS, followed by fluorescence quenching at longer exposure with HS (>30 min). It was also observed that the electrophoretic mobility of QDs increases with increasing concentration of HS, suggesting an increase in the ratio in charge to hydrodynamic size of the nanoparticles. To determine if the QDs degraded upon interaction with HS, the QD–HS mixtures were dialyzed to separate free Cd<sup>2+</sup> from intact QDs, followed by analysis of the solutions using inductively coupled plasma-mass spectrometry. Results suggested that degradation of QDs in the presence of HS did not occur within the period of incubation.



## INTRODUCTION

Quantum dots (QD) are semiconductor nanoparticles that are finding an increasing number of applications in modern society, ranging from their use as fluorescent probes in cellular imaging and biological assays, to materials in solar cells.<sup>1–5</sup> These nanoparticles exhibit quantum size effects that influence their absorption/emission properties<sup>6</sup> and extinction coefficient.<sup>7</sup> The use of QDs as labeling tools for fluorescence measurements has several advantages over organic dyes. These include high fluorescence quantum yield in both visible and near-infrared region, broad absorption spectra that allow a wide selection range of excitation wavelengths, narrow emission band, large molar absorption coefficients, and high photostability.<sup>8,9</sup> Some of the potential applications of commercially available water-soluble carboxylic or amine-conjugated CdSe/ZnS QDs are as fluorescence resonance energy transfer-based biosensor,<sup>10,11</sup> for imaging and drug delivery,<sup>12,13</sup> and as nanocomposite material with potential light emitting diodes and solar cell applications.<sup>14</sup>

Humic substances (HS), consisting of a collection of diverse high and low molecular weight molecules including humic acids (HA) and fulvic acids (FA), influence the fate and transport of pollutants.<sup>15,16</sup> Both metals<sup>17</sup> and organic pollutants<sup>18</sup> can bind to HS and affect their environmental processes. Recent studies have demonstrated that HS can affect the aggregation and stabilization behavior of gold<sup>19</sup> and C<sub>60</sub> nanoparticles.<sup>20</sup> For

example, the presence of HS can facilitate the phase transfer of water-insoluble QDs from a hydrophobic solvent into an aqueous phase.<sup>21</sup>

Despite the increasing popularity of QDs, there is a growing concern about the potential negative ecological effects of these nanomaterials. The ecotoxicity of QDs depends on a number of factors, such as the extent at which the toxic inorganic components could leach out, the surface chemistry of the coating material, aggregation, size, and ability to induce formation of reactive oxygen species.<sup>22–27</sup> Cytotoxicity arising from surface oxidation and release of the toxic inorganic constituents can be minimized by using a protective coating.<sup>22</sup> Several QDs that are commercially available contain various types of protective coating; however, it has been shown that the coating does not exclude it from being cytotoxic. For instance, thrombosis was observed in mice injected with carboxyl-capped QDs,<sup>28</sup> while in a different study, PEG-COOH- and PEG-amine-coated CdSe/ZnS QDs exhibited toxicity to human epidermal cells.<sup>29</sup> The interactions of QDs with test organisms in the environment showed that, at extreme pH conditions, weathering of QDs can take place,

**Received:** September 11, 2010

**Accepted:** February 14, 2011

**Revised:** February 8, 2011

**Published:** March 07, 2011

leading to bacterial cell death due to the toxicity of released cadmium and selenite ions.<sup>30</sup> Recently, assimilation of carboxylate functionalized QDs by *Ceriodaphnia dubia*, a crustacean, fed with algae exposed to QDs was observed, indicating potential for bioconcentration of QDs in certain species.<sup>31</sup> Finally, membrane damage to a metal-resistant bacteria when exposed to carboxylated or aminated QDs was reported; this damage was mitigated in the presence of HA.<sup>32</sup>

Because of the critical role of HS in facilitating transport and toxicity of QDs in the environment, it is important to have an understanding on how water-soluble QDs can interact with HS. The interactions of QDs with HS may be investigated by relating changes in the electrophoretic mobilities and fluorescence spectra with varying HS concentrations using capillary electrophoresis (CE). The CE is a high-resolution separation technique based on differential electromigration of species inside a capillary tube. It has the advantages of providing highly efficient and rapid separations. The small sample volume requirement is also advantageous in cases with limited samples. Binding of QDs with macromolecules such as proteins, surfactants, and natural organic matter (NOM) in the environment can be determined using CE because interactions with these macromolecules will result in changes in the hydrodynamic size of QDs. In recent years, CE has emerged as a powerful tool for characterizing and separating QDs and other nanoparticles. Several studies have demonstrated that CE separation of QDs with different organic surface ligands is possible based primarily on surface charge distribution.<sup>33–37</sup> Recent reports have shown successful applications of CE in monitoring the interaction between two bioconjugated QDs,<sup>36</sup> in characterizing QDs and bioconjugated QDs,<sup>34,38,39</sup> and in determining the size of QDs.<sup>33</sup> CE has been used to estimate binding constants by monitoring the changes in the electrophoretic mobility of the analyte in the presence of complexing agents in the buffer.<sup>40</sup>

To date, the potential of CE in the characterization of the environmental behavior of nanoparticles has not been explored. Hence, this present study investigates the application of CE with laser-induced fluorescence (LIF) detection to monitor the changes in the fluorescence intensities and electrophoretic mobilities of water-soluble QDs in the presence of HA and FA. Charge-to-size ratio is the fundamental parameter that determines electrophoretic mobility in CE, and, therefore, mobility can be correlated to the size of QDs. This study examines the potential of CE as a tool to monitor changes in QD size brought about by environmental degradation or by interaction with NOM.

## EXPERIMENTAL SECTION

**Chemicals.** Suwannee River Humic Acid Standard II (SRHA) and Suwannee River Fulvic Acid Standard II (SRFA) were purchased from International Humic Substances Society (St. Paul, MN). Stock solutions (1000 ppm) of the HS were prepared in water by sonication for 1 h, then filtration through a 0.45  $\mu\text{m}$  polyethersulfone syringe filter (Sun-Sri, Rockwood, TN). Two kinds of QDs were used in this work. EviTag QDs were composed of CdSe/ZnS/PEG lipid coating with carboxyl functionality emitting at  $580 \pm 10$  nm, a hydrodynamic radius of 25 nm, and a core molecular weight of 29 kD (QDCOOH); they were obtained from Evident Technologies (Troy, NY). eFluor 650<sup>NC</sup> (amine) QDs composed of CdSe/ZnS/lipid coating with an amine functionality emitting at 650 nm and a particle diameter of 20–25 nm with the PEG (QDNH<sub>2</sub>) were purchased from

eBioscience, Inc. (San Diego, CA). The QDs were shipped in water at 12  $\mu\text{M}$  for QDCOOH and 10  $\mu\text{M}$  for QDNH<sub>2</sub>. Stock solutions of the QDs were prepared in water and stored at 4 °C. Samples for CE analysis were diluted in 20% of the run buffer. 3-Cyclohexylamino-1-propane sulfonic acid (CAPS) was purchased from Alfa Aesar (Ward Hill, MA). CAPS buffer solution was prepared and adjusted to desired pH using 0.1 M NaOH. The buffer solution was filtered through a 0.45  $\mu\text{m}$  VWR Nylon syringe filter (West Chester, PA). BODIPY 493/503 (4,4-difluoro-1,3,5,7,8-pentamethyl-4-bora-3a,4a-diaza-s-indacene) was purchased from Invitrogen Corp. (Carlsbad, CA). A stock solution of BODIPY was prepared in methanol at 1  $\mu\text{M}$ . Mesityl oxide was purchased from Sigma-Aldrich (St. Louis, MO). The water used throughout was obtained from a Barnstead Easypure II ultrapure water purification system (ThermoScientific, Waltham, MA).

**Experimental Design.** Two setups of the CE experiments were performed to monitor the changes in the fluorescence intensities of QDs when exposed to either SRHA or SRFA. The first setup involved injecting QDs into the CE system equipped with LIF detector and using a separation buffer that contained SRHA or SRFA. Five injections were performed for each QD:HS mole ratio. The weight-averaged molecular weight used to calculate the mole ratios was 3409 Da for SRHA and 2114 Da for SRFA, which were determined by size exclusion chromatography with dissolved organic carbon analyzer as detector.<sup>41</sup> The net electrophoretic mobility of the QD was determined from the difference between the electroosmotic mobility and the observed electrophoretic mobility of the QD. The electroosmotic mobility was estimated using the change in current method.<sup>42</sup> The second setup of the CE experiment involved incubating QDs with SRHA or SRFA at different mole ratios before injecting into the CE-LIF system. The incubation time of QDs with SRHA or SRFA was 2, 8, 15, 22, 28, 35, and 41 min.

Changes in the fluorescence intensities of QDs in the presence of SRHA or SRFA were measured using a Cary Eclipse fluorescence spectrophotometer (Varian Inc., Palo Alto, CA) at an excitation wavelength of 488 nm. One nanomolar of QDCOOH or 0.5 nM of QDNH<sub>2</sub> was mixed with 340 ppb SRHA or 211 ppb SRFA using either water or 10 mM CAPS, pH 10 as solvent. This gives a ratio of 1:100 QD:HS for QDCOOH and 1:200 for QDNH<sub>2</sub>. Fluorescence measurements were taken 1 min and 3 h after mixing.

Dialysis was performed to separate QDs from the inorganic components to investigate if weathering of QDs occurred. Details of the dialysis procedure are provided in the Supporting Information. To quantify the cadmium concentration in the retentate (what remained inside the dialysis membrane) and the dialysate (what came out of the membrane), the solutions were placed in polyethylene bottles that contain 0.2% HNO<sub>3</sub> and sent for cadmium analysis using inductively coupled plasma-mass spectrometry (ICP-MS) at Activation Laboratories Ltd. (Ancaster, Ontario, Canada).

**Instrumentation.** CE separations were performed using a Beckman Coulter P/ACE MDQ CE system equipped with an on-column LIF or UV detection system and a 32 Karat version 7 software (Fullerton, CA). For LIF detection, an argon ion 488 nm laser module was used as the excitation source. The emitted light was collected after passing through a 488 nm notch filter (Beckman Coulter, Inc.) and a bandpass filter. A 520 nm bandpass filter (Beckman Coulter, Inc.) was used for BODIPY and/or a 585 or 655 nm bandpass filter (Omega Optical, Brattleboro, VT) for detecting QDCOOH or QDNH<sub>2</sub>,

respectively. The separation was performed using a fused silica capillary (50  $\mu\text{m}$  ID  $\times$  30 cm total length) with an effective length of 20 cm (Polymicro Technologies, Phoenix, AZ). The detection window was made by burning  $\sim 0.3$  cm portion of the polyimide coating of the capillary. The capillary was conditioned with 0.1 M NaOH for 20 min, followed by water for 5 min, then separation buffer for 10 min. The separation buffer was 10 mM CAPS, pH 10. The capillary was equilibrated by applying 15 kV for 10 min before starting the sample analysis. A buffer and water injection were performed before the samples. Between analysis, the capillary was washed with the separation buffer for 1.5 min. Hydrodynamic injection at 0.5 psi for 5 s was employed. The separation voltage was 15 kV. The temperature of the column was maintained at 20  $^{\circ}\text{C}$ .

## RESULTS AND DISCUSSION

**Effect of SRHA or SRFA on the Electrophoretic Mobility of QDs.** Two commercially available QDs were used as models to investigate the effect of surface capping on the interaction of nanoparticles with HS. The QDs used in this study contained the same inorganic components for the core and shell but differed in the surface functionality and size. The electropherograms of the QDs using LIF detection and BODIPY as neutral marker are shown in Figure 1. The QDs migrated after the neutral species, indicating that both QDs had a net negative charge; their electrophoretic mobilities were  $(-1.23 \pm 0.02) \times 10^{-4} \text{ cm}^2/(\text{V} \cdot \text{s})$  ( $n=3$ ) for QDNH<sub>2</sub> and  $(-1.09 \pm 0.03) \times 10^{-4} \text{ cm}^2/(\text{V} \cdot \text{s})$  ( $n=5$ ) for QDCOOH. While carboxylic groups in QDCOOH are negatively charged at pH 10, the close migration time of QDs to the neutral marker indicates that the number of negatively charged functional groups is small relative to the size of the nanoparticle. Similarly, QDNH<sub>2</sub> migrated immediately after the neutral marker, implying that it has a net negative charge at the pH used. No change in the net charge of QDNH<sub>2</sub> was observed when the pH was lowered to 6 using 10 mM 2-(*N*-morpholino)-ethanesulfonic acid (MES). This observation agreed with previous reports that aminated QDs obtained from Evident Technologies (now owned by eBioscience, which produces eFluors) have negatively charged surface.<sup>28,38</sup>

The electropherograms of SRFA and SRHA were obtained using CE with a UV detector operated at 254 nm, using mesityl oxide as neutral marker (Figure 1). Both SRFA and SRHA migrated after the neutral marker, indicating that these substances have net negative charge under the conditions used; this was expected because HS contains carboxylic and phenolic groups that can be deprotonated at pH 10. The broadness of the HS peak is attributed to the polydispersity of HS.<sup>43,44</sup>

In CE, the interaction between a solute (QD) and a ligand (HS) can be monitored by measuring the changes in the electrophoretic mobility ( $\mu_{\text{ep}}$ ) of the solute. In this study, the changes in the  $\mu_{\text{ep}}$  of QDs were monitored by injecting a constant amount of QDs into the CE column containing various amounts of SRHA or SRFA in the separation buffer. The  $\mu_{\text{ep}}$  was calculated as the difference between the observed electrophoretic mobility ( $\mu_{\text{app}}$ ) and electroosmotic mobility ( $\mu_{\text{eo}}$ ). The  $\mu_{\text{eo}}$  was determined using the equation:

$$L_t/Vt \quad (1)$$

where  $L_t$  is the total length of the capillary,  $V$  is the applied voltage, and  $t$  is the time when an abrupt change in the current is

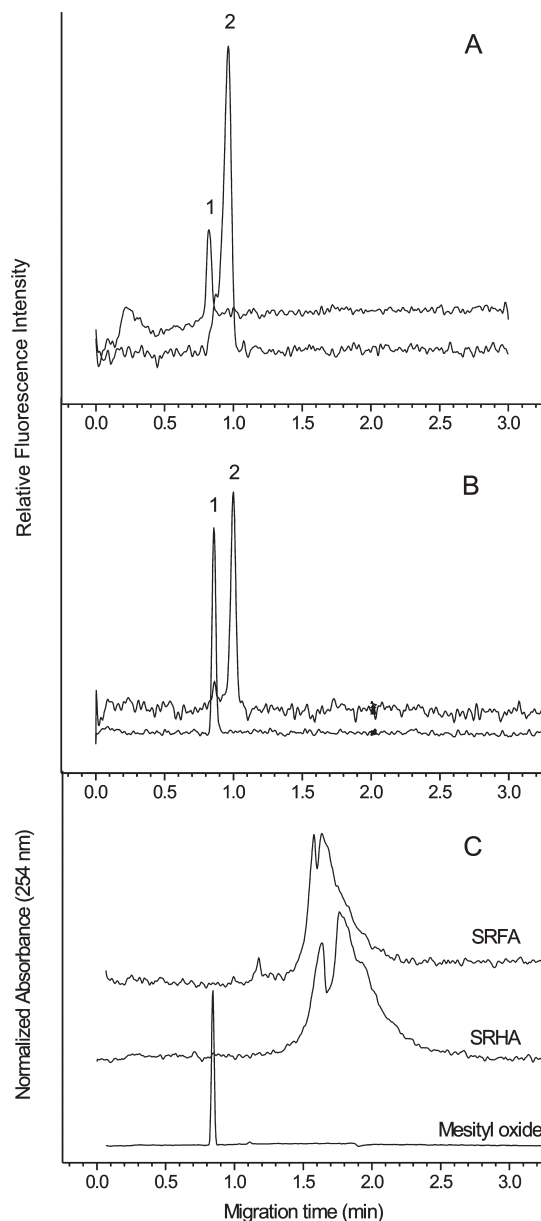


**Figure 1.** Electropherograms of (A) QDNH<sub>2</sub> (peak 2) and (B) QDCOOH (peak 2) with BODIPY as the neutral marker (peak 1) and (C) SRHA, SRFA, and mesityl oxide as the neutral marker. The CE conditions are as follows:  $L_t$ , 30 cm ( $L_d$ , 20 cm)  $\times$  50  $\mu\text{m}$ ; separation buffer, 10 mM CAPS, pH 10; applied voltage, 15 kV; capillary temperature, 20  $^{\circ}\text{C}$ ; injection, 5 s at 0.5 psi. LIF detection wavelengths are  $\lambda_{\text{ex}} = 488 \text{ nm}$ ,  $\lambda_{\text{em}} = 585 \text{ nm}$  (QDCOOH) or 655 nm (QDNH<sub>2</sub>), and 520 nm (Bodipy). The UV detector was set at 254 nm.

observed.<sup>42</sup> The  $\mu_{\text{app}}$  was calculated using the equation:

$$L_t L_d / V t_m \quad (2)$$

where  $L_d$  is the length from the injection end to the detector, and  $t_m$  is the migration time of the analyte. The  $\mu_{\text{ep}}$  of QDCOOH and QDNH<sub>2</sub> increased as the concentration of the SRHA or SRFA in the buffer increases. It was noted that the current values decreased by 0.3  $\mu\text{A}$  from 2.5  $\mu\text{A}$  with the addition of HS, implying that there is a change in the viscosity of the buffer. To compensate for the slight changes in the electroosmotic flow (EOF) due to addition of



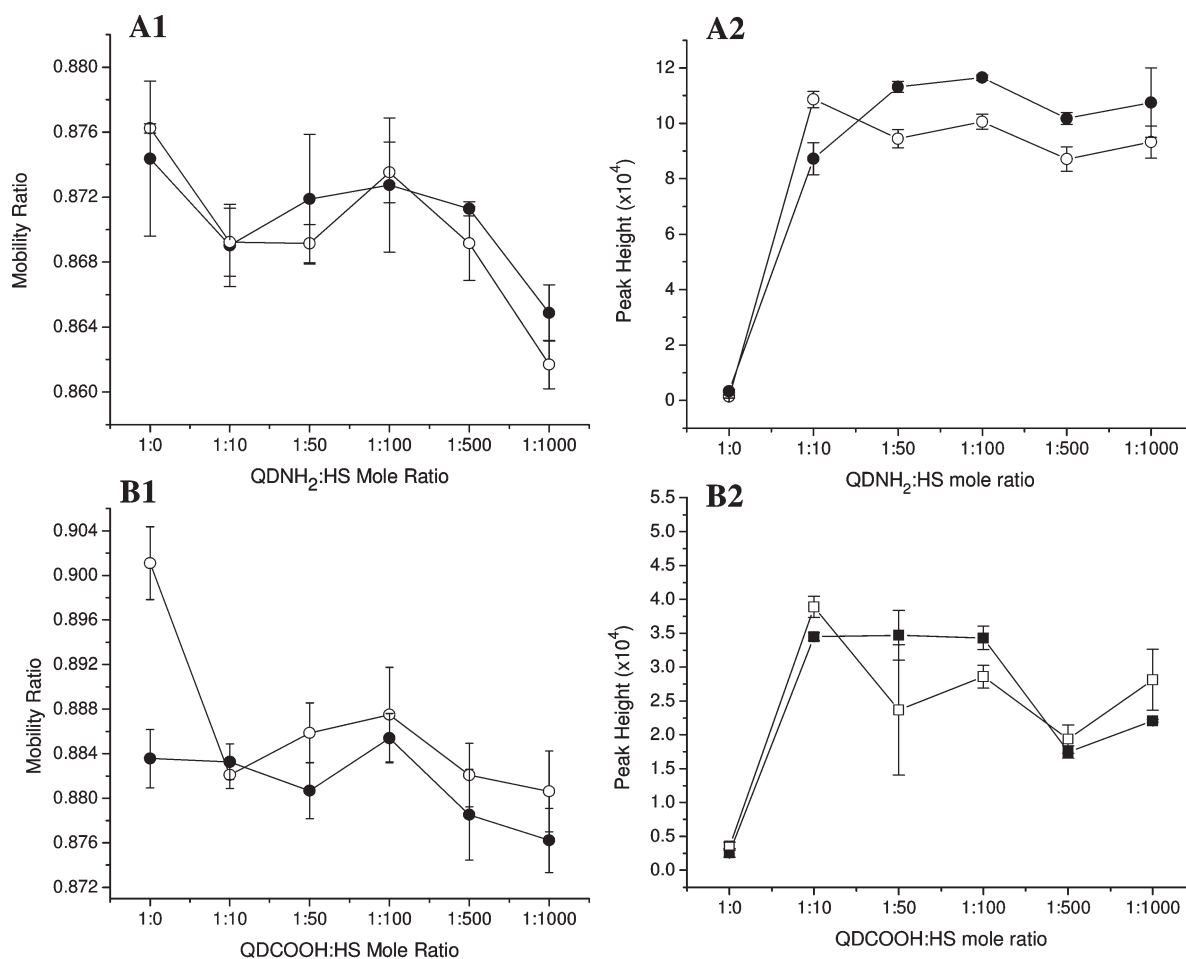


**Figure 2.** Effect of increasing amount of SRFA (■ or ●) or SRHA (□ or ○) in the separation buffer on the (1) mobility ratio and (2) peak height of QDNH<sub>2</sub> (A) and QDCOOH (B). The CE and LIF conditions are the same as described in Figure 1. Samples are 30 nM QD in 20% buffer. The separation buffer contains 0, 0.6, 3, 6, 30, and 60 ppm SRFA or 0, 1, 5, 10, 50, and 100 ppm SRHA corresponding to the QD:HS mole ratios of 1:0, 1:10, 1:50, 1:100, 1:500, and 1:1000, respectively. There are five injections per QD:HS mole ratio. A *t* test was performed at 95% confidence level to determine significance. Figure 2A1 reprinted from reference 59, with permission from Elsevier.

HS, mobility ratios were used,<sup>45</sup> which can better represent the interactions occurring between QD and HS. Theoretically, mobility ratio is independent of the operating voltage, length of the capillary, and viscosity of the running buffer.<sup>46</sup> The mobility ratio is calculated using the equation:

$$\mu_{\text{app}}/\mu_{\text{eo}} \quad (3)$$

The mobility ratios for QDNH<sub>2</sub> and QDCOOH are shown in Figure 2 (A1 and B1). The mobility ratios of QDs injected into the buffer with SRHA are significantly different from the sample without SRHA added. On the other hand, for SRFA, only QD:HS mole ratios of 1:500 and 1:1000 for QDCOOH and 1:1000 for QDNH<sub>2</sub> showed significant differences from 1:0. However, a decreasing trend can be observed for both QDs in SRFA and SRHA. This indicates that QD mobilities are increasing toward the anode (away from the detector) with increasing concentration of the SRFA or SRHA in the buffer. Because SRHA and SRFA are negatively charged at the conditions used, its interaction with QDs would be expected to add to the negatively charged character of the QDs, thereby increasing its mobility toward the anode. The representative electropherograms of QD:

HS at each mole ratio are shown in Figure S1 (Supporting Information).

Under the conditions used in the experiments, separation between free QDs and QD–HS complex was not observed in the electropherograms when QDs were mixed with SRHA or SRFA. The absence of two distinct peaks could mean that either all of the QDs are present as QD–HS complex or the difference in the charge-to-size ratios between the free and complexed QD species was very small to be separated under these conditions. The hydrodynamic sizes of the QDs reported by the manufacturer are 25 nm for the QDCOOH and 20–25 nm for the QDNH<sub>2</sub>. The reported hydrodynamic size of SRHA is 1.7 nm, while SRFA is 1.5 nm at pH > 7.<sup>47</sup> Because of the small size of SRHA or SRFA in comparison to the size of the QDs, the separation efficiency of the CE under these conditions was not enough to distinguish between the QD–HS complex and QDs due to negligible size difference between the two species. There are several things that can be done to improve separation in CE: increase the column length, change the background electrolyte to something that will provide slower electroosmotic flow without affecting the fluorescence of QDs, decrease the temperature, and decrease the applied voltage. However, as long as the changes in the

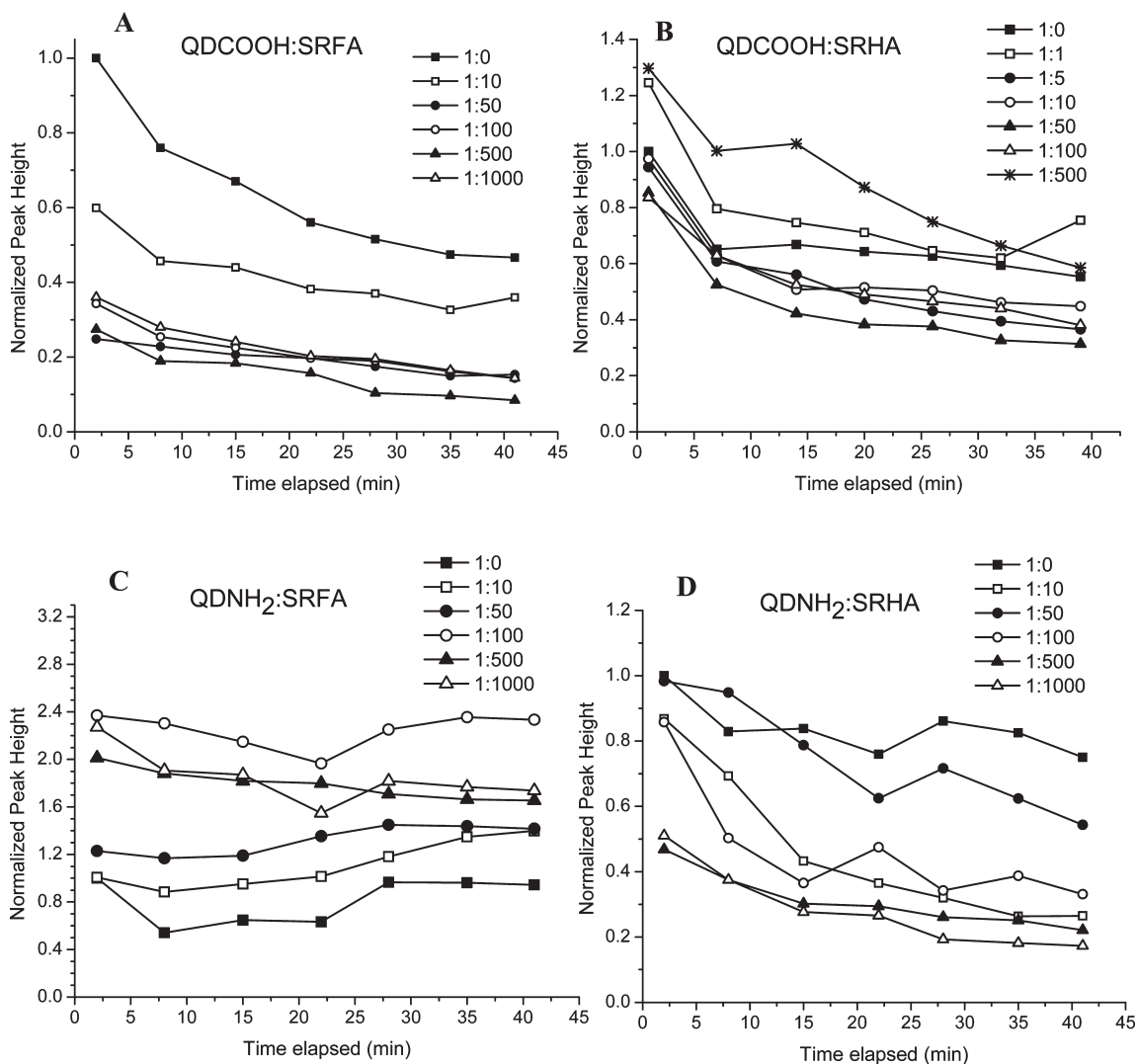


**Figure 3.** Profile of fluorescence peak height showing the effect of SRFA and SRHA on QDCOOH (A and B) and QDNH<sub>2</sub> (C and D) at increasing exposure time. The legends refer to the mole ratios of QD:SRFA or QD:SRHA. QDCOOH:SRFA samples contained 15 nM QD with 0, 0.3, 1.6, 3, 16, and 32 ppm SRFA in 20% buffer, while QDCOOH:SRHA samples had 20 nM QD with 0, 0.07, 0.35, 0.7, 3.5, 7, and 35 ppm SRHA in 60% buffer. QDNH<sub>2</sub>:SRFA samples contained 30 nM QD with 0, 0.6, 3.2, 6, 32, and 63 ppm SRFA, while QDNH<sub>2</sub>:SRHA samples had 6 nM QD with 0, 0.2, 1, 2, 10, and 20 ppm SRHA in 20% buffer. The CE and LIF conditions are the same as described in Figure 1. Peak height is normalized to the peak height of the first injection of the 1:0 sample. Assuming a linear curve, the average slopes of the QDHS mole ratios were significantly different from zero for (A), (B), and (D) as determined from the *t* test at 95% confidence level, indicating that the fluorescence signal is changing with time.

electroosmotic mobility of the QDs can be measured, complete separation is not necessary. On the other hand, if the complexation constant between QD and HS is very large, then it is reasonable to assume that free QDs are negligible.

**Effect of SRHA or SRFA on the Fluorescence of QDs.** The size-dependent fluorescence emission of QDs is an important parameter that can be used to determine the integrity of these nanomaterials. In the second setup of the CE experiments, known amounts of QDs were premixed with SRHA or SRFA, then injected into the CE at various times. A general decrease in the fluorescence signal of the QDs was observed upon mixing with either SRFA or SRHA, except for QDNH<sub>2</sub>–SRFA mixture (Figure 3). While a previous study reported that the fluorescence of individual particles and the hydrodynamic radius of an amine or carboxyl-PEG-QD did not change in the presence of HA, as determined by fluorescence correlation spectroscopy (FCS),<sup>32</sup> our study showed otherwise and can be attributed to differences

in the experimental conditions. Previous studies have demonstrated similar reduction in the fluorescence of carboxyl-PEG-coated CdSe/ZnS QDs upon interaction with microalga.<sup>48</sup> We inferred that aggregation of QDs in the presence of SRHA or SRFA did not occur based on the absence of spikes in the electropherogram, which would be observed if aggregates are present.<sup>49</sup> In Figure 3A,B,D, a reduction in the peak height of QDs over time is noticeable in the sample that does not contain SRHA or SRFA, which was more pronounced for QDCOOH. When the SRHA fluorescence was monitored, no corresponding increase in its fluorescence was observed upon mixing with QDs, implying that the decrease in QD luminescence did not affect the emission from HS (Figure S2). The interaction of the HA and FA with the surface functionalities of the QDs<sup>50</sup> by overcoating the QD could have caused these changes in fluorescence intensities. This observation is consistent with the report that quenching of QD signal can result from the changes in the structure of QD

surface.<sup>51</sup> The QDNH<sub>2</sub>–SRFA, on the other hand, exhibited opposite behavior (Figure 3C). An increasing concentration of SRFA resulted in the corresponding increase in peak height of QDs up to 1:100 QD:SRFA mole ratio. Additional increase in the SRFA concentration did not elicit further increase in the QD signal. The signal did not appear to change considerably with time. While the exact cause of this opposing behavior is unclear at this time, we hypothesize that the initial increase in fluorescence of QDNH<sub>2</sub> may be due to the prevention of QDNH<sub>2</sub> adsorption on the capillary wall by the presence of small amounts of SRFA (up to 1:100 QDNH<sub>2</sub>:SRFA) that initially coat the wall. Consequently, more QD particles are detected by LIF. A previous study by Slaveykova et al.<sup>52</sup> using FCS reported that the fluorescence of individual particles of QDCOOH and QDNH<sub>2</sub> was not affected by 15 mg C L<sup>-1</sup> SRHA. However, further increase in QDNH<sub>2</sub> can overcoat the QD,<sup>50</sup> resulting in a reduction in the fluorescence intensity.

Despite the fact that the QDs used in these experiments contained a shell and polymer that protect the core material, there are studies that have shown reduction of QD fluorescence even with the shell and polymer coating. For example, fluorescence of polymer encapsulated core/shell QDs (CdSe/CdS/ZnS) was quenched when exposed to hypochlorous acid, which may have oxidized the sulfur and selenium ions and forms defect sites for nonradiative decay.<sup>52</sup> Quenching of core/shell QDs (CdSe/ZnS) was also observed when titrated with pyridyl-functionalized porphyrin, due to electron tunneling through the ZnS barrier into the surface.<sup>53</sup> It should be noted that the pH condition used in the present study is high, and that results obtained at lower pH may be different due to HS aggregation at low pH.<sup>47</sup> Preliminary studies were conducted to examine suitability of different buffers with different pHs as run buffers in CE. It was found that the peak and signal intensities of QDs (without HS) were higher at high pH (data not shown), demonstrating the sensitivity of QD fluorescence to its chemical environment. Low pH has been found to promote formation of dark QDs (nonfluorescent),<sup>54</sup> which may have caused the detection problems encountered at pH 5 in this study. A pH 10 buffer was selected in the present study to minimize HS adsorption on the capillary wall.<sup>55</sup>

In the first setup of CE experiments, increasing amounts of SRHA or SRFA were mixed with the running buffer, while injecting a constant amount of QDs. This setup was designed to investigate the instantaneous effect of HS on the fluorescence intensities and electrophoretic mobilities of QDs. The fluorescence intensities of QDs were enhanced initially (Figure 2A2 and B2) in the presence of SRHA or SRFA in the buffer. A sharp increase in the peak height of the QD signal was observed at lower concentrations of the SRHA or SRFA; then the peak height leveled off at higher concentrations of the SRHA or SRFA, which can be due to saturation. The results from these experiments contradicted the results shown in Figure 3 where quenching of the signal was observed. In the setup for Figure 2A2 and B2, the exposure of the QDs to SRHA or SRFA occurred from injection to detection only, which is a short period to allow overcoating of QDs with the SRHA or SRFA. In other words, at the onset of the interaction, SRHA and SRFA generate QD fluorescence enhancement, while at longer periods of SRHA and SRFA exposure, QD quenching takes place. Steady-state fluorescence measurements were also performed on QD–SRHA and QD–SRFA mixtures dissolved in water and 10 mM CAPS, at pH 10, to mimic the CE conditions, and the results are presented in the

Supporting Information (Figures S3 and S4). The QDCOOH and QDNH<sub>2</sub> have emission peak maxima at 588 and 657 nm, respectively (Figure S3). The fluorescence intensities were normalized to the highest intensity. The maximum emission wavelength did not change in the presence of SRHA or SRFA, indicating that the structural integrity, specifically the band gap, of the fluorescing particles was preserved. In contrast, QDs that do not have the ZnS shell and PEG coating can exhibit blue-shifted emission in the presence of HA.<sup>21</sup>

**Application of CE in Determining Cd<sup>2+</sup> Release in the Environment.** The changes in fluorescence intensities of QDs upon interaction with HS were further investigated by dialysis of the QD–SRHA mixture, followed by ICP–MS analysis of retentate and dialysate to quantify any leaching of the Cd<sup>2+</sup> core metal (Table S1). A 50 kD membrane was used to allow dissolved inorganic components of QDs to pass through the membrane, but not the QDs or SRHA. A separate dialysis experiment showed retention of SRHA inside the 50 kD membrane. This was unexpected because the reported molecular weight of SRHA is approximately 3 kD,<sup>41</sup> which means that SRHA should come out of the dialysis membrane. It is possible that aggregation of SRHA occurred, preventing its transport through the membrane. The amount of Cd<sup>2+</sup> in the retentate of dialyzed QD solution (6.8 μg for QDCOOH and 54 μg for QDNH<sub>2</sub>) and in a freshly prepared (undialyzed) QD solution (9.2 μg for QDCOOH and 62 μg for QDNH<sub>2</sub>) showed a slight difference, which can be attributed to adsorption of some QDs unto the membrane. A small amount of Cd<sup>2+</sup> was detected in the dialysate of the freshly prepared QDs (0.0064 μg for QDCOOH and 0.0028 μg for QDNH<sub>2</sub>), which indicates the presence of free Cd<sup>2+</sup> in the purchased QD solutions. Otherwise, the Cd<sup>2+</sup> was retained in the membrane for the QD–SRHA samples after dialysis, suggesting that the QDs did not degrade in the presence of SRHA. When a similar amount of Cd<sup>2+</sup> found in QDs was dialyzed with SRHA, most of the Cd<sup>2+</sup> was detected in the dialysate (77% for QDCOOH and >82% for QDNH<sub>2</sub>), which means that if degradation of QDs occurred, the Cd<sup>2+</sup> should be detected in the dialysate. The results suggest the possibility that at least within the 24 h exposure used in these studies, QDs can resist degradation even in the presence of SRHA and SRFA.

The goal of this Article was to determine if CE is a suitable tool to investigate the interactions of QDs with HS by relating changes in the electrophoretic mobilities and fluorescence intensities of QDs upon exposure to varying HS concentrations. We observed that the electrophoretic mobilities generally increase with increasing HS concentration in the background electrolyte, but that the maximum emission wavelength did not change. This observation supports the hypotheses presented in earlier studies indicating that HS overcoat the QDs (hence the change in electrophoretic mobility), but that the core materials are not leached or dissolved upon interaction with HS (hence there is no change in the maximum emission wavelength and spectra of QDs). The protective coating of QDs plays a big role in the stability of the nanoparticles. It is expected that the observed stability of the surface coating and the shell material will prevent release of the core components into the environment. However, longer exposure times in the environment may produce different results and need to be investigated.

Even though the QDs in this present study did not show evidence of degradation, different environmental conditions such as pH, sunlight, and agents that promote oxidation–reduction reactions can certainly influence the stability of QDs. In addition,



different experimental conditions and the type of HS can also influence the aggregation/disaggregation of HS,<sup>56,57</sup> which in turn might affect its interaction with QDs. In these types of studies, a combination of analytical techniques will be needed. While the use of CE with LIF can provide information on the changes in the electrophoretic mobilities and fluorescence intensities of QDs, the LIF detection cannot provide quantitative information on the amount of free cadmium or zinc ions. Therefore, a combination of data from ICP-MS and CE-LIF analysis could better facilitate the characterization of QDs in the environment. In addition, FCS will be useful in determining simultaneously both the number and the fluorescence intensity of single QD particles upon interaction with HS, as has been demonstrated previously by Slaveykova et al.<sup>32</sup> Nevertheless, the electrophoretic mobilities of QDs as measured by CE can be correlated to the size of QDs based on two methods: first, by using a calibration curve obtained from the electrophoretic mobilities of QDs with known sizes,<sup>33</sup> and second, by using a mathematical expression based on zeta potential.<sup>58</sup> On the basis of this study and as discussed in a recent review,<sup>59</sup> changes in QD size brought about by environmental degradation or by interaction with NOM in the environment may be potentially monitored by CE.

## ■ ASSOCIATED CONTENT

**S Supporting Information.** Materials and methods, and additional figures and table. This material is available free of charge via the Internet at <http://pubs.acs.org>.

## ■ AUTHOR INFORMATION

### Corresponding Author

\*Phone: (716) 645-4220 (D.S.A.); (716) 645-4213 (L.A.C.). Fax: (716) 645-6963. E-mail: [dianaaga@buffalo.edu](mailto:dianaaga@buffalo.edu) (D.S.A.); [lacoloni@buffalo.edu](mailto:lacoloni@buffalo.edu) (L.A.C.).

## ■ ACKNOWLEDGMENT

This material is based upon work supported by the Environmental Protection Agency (EPA) Grant No. R833861. The research described in this work has not been subjected to any peer and policy review by the EPA and does not necessarily reflect the views of the agency; therefore, no official endorsement should be inferred. M.D.C. also acknowledges the Mark Diamond Research Fund (University at Buffalo) for some funding to purchase some of the chemicals used in this research.

## ■ REFERENCES

- (1) Li, H.; Han, C. Sonochemical synthesis of cyclodextrin-coated quantum dots for optical detection of pollutant phenols in water. *Chem. Mater.* **2008**, *20*, 6053–6059.
- (2) Alivisatos, A. P.; Gu, W.; Larabell, C. Quantum dots as cellular probes. *Annu. Rev. Biomed. Eng.* **2005**, *7*, 55–76.
- (3) Medintz, I. L.; Uyeda, H. T.; Goldman, E. R.; Mattoussi, H. Quantum dot bioconjugates for imaging, labelling and sensing. *Nat. Mater.* **2005**, *4*, 435–446.
- (4) Leschkes, K. S.; Divakar, R.; Basu, J.; Enache-Pommer, E.; Boercker, J. E.; Carter, C. B.; Kortshagen, U. R.; Norris, D. J.; Aydil, E. S. Photosensitization of ZnO nanowires with CdSe quantum dots for photovoltaic devices. *Nano Lett.* **2007**, *7*, 1793–1798.
- (5) Frasco, M. F.; Chaniotakis, N. Semiconductor quantum dots in chemical sensors and biosensors. *Sensors* **2009**, *9*, 7266–7286.

- (6) Alivisatos, A. P. Semiconductor clusters, nanocrystals, and quantum dots. *Science* **1996**, *271*, 933–937.
- (7) Yu, W. W.; Qu, L.; Guo, W.; Peng, X. Experimental determination of the extinction coefficient of CdTe, CdSe, and CdS nanocrystals. *Chem. Mater.* **2003**, *15*, 2854–2860.
- (8) Resch-Genger, U.; Grabolle, M.; Cavaliere-Jaricot, S.; Nitschke, R.; Nann, T. Quantum dots versus organic dyes as fluorescent labels. *Nat. Methods* **2008**, *5*, 763–775.
- (9) O'Farrell, N.; Houlton, A.; Horrocks, B. R. Silicon nanoparticles: Application in cell biology and medicine. *Int. J. Nanomed.* **2006**, *1*, 451–472.
- (10) Suzuki, M.; Husimi, Y.; Komatsu, H.; Suzuki, K.; Douglas, K. T. Quantum dot FRET biosensors that respond to ph, to proteolytic or nucleolytic cleavage, to DNA synthesis, or to a multiplexing combination. *J. Am. Chem. Soc.* **2008**, *130*, 5720–5725.
- (11) Dennis, A. M.; Sotito, D. C.; Mei, B. C.; Medintz, I. L.; Mattoussi, H.; Bao, G. Surface ligand effects on metal-affinity coordination to quantum dots: Implications for nanoprobe self-assembly. *Bioconjugate Chem.* **2010**, *21*, 1160–1170.
- (12) Bagalkot, V.; Zhang, L.; Levy-Nissenbaum, E.; Jon, S.; Kanto, P. W.; Langer, R.; Farokhzad, O. C. Quantum dot-aptamer conjugates for synchronous cancer imaging, therapy, and sensing of drug delivery based on bi-fluorescence resonance energy transfer. *Nano Lett.* **2007**, *7*, 3065–3070.
- (13) Bothun, G. D.; Rabideau, A. E.; Stoner, M. A. Hepatoma cell uptake of cationic multifluorescent quantum dot liposomes. *J. Phys. Chem. B* **2009**, *113*, 7725–7728.
- (14) Kehlbeck, J. D.; Hagerman, M. E.; Cohen, B. D.; Eliseo, J.; Fox, M.; Hoek, W.; Karlin, D.; Leibner, E.; Nagle, E.; Nolan, M.; Schaefer, I.; Toney, A.; Topka, M.; Uluski, R.; Wood, C. Directed self-assembly in laponite/CdSe/polyaniline nanocomposites. *Langmuir* **2008**, *24*, 9727–9738.
- (15) Steelink, C. Investigating humic acids in soils. *Anal. Chem.* **2002**, *74*, 326A–333A.
- (16) Sutton, R.; Sposito, G. Molecular structure in soil humic substances: The new view. *Environ. Sci. Technol.* **2005**, *39*, 9009–9015.
- (17) Bidoglio, G.; Ferrari, D.; Selli, E.; Sena, F.; Tamborini, G. Humic acid binding of trivalent Ti and Cr studied by synchronous and time-resolved fluorescence. *Environ. Sci. Technol.* **1997**, *31*, 3536–3543.
- (18) Uhle, M. E.; Chin, Y.-P.; Aiken, G. R.; McKnight, D. M. Binding of polychlorinated biphenyls to aquatic humic substances. The role of substrate and sorbate properties on partitioning. *Environ. Sci. Technol.* **1999**, *33*, 2715–2718.
- (19) Diegoli, S.; Manciu, A. L.; Begum, S.; Jones, I. P.; Lead, J. R.; Preece, J. A. Interaction between manufactured gold nanoparticles and naturally occurring organic macromolecules. *Sci. Total Environ.* **2008**, *402*, 51–61.
- (20) Xie, B.; Xu, Z.; Guo, W.; Li, Q. Impact of natural organic matter on the physicochemical properties of aqueous C<sub>60</sub> nanoparticles. *Environ. Sci. Technol.* **2008**, *42*, 2853–2859.
- (21) Navarro, D. A. G.; Watson, D. F.; Aga, D. S.; Banerjee, S. Natural organic matter-mediated phase transfer of quantum dots in the aquatic environment. *Environ. Sci. Technol.* **2009**, *43*, 677–682.
- (22) Derfus, A. M.; Chan, W. C. W.; Bhatia, S. N. Probing the cytotoxicity of semiconductor quantum dots. *Nano Lett.* **2004**, *4*, 11–18.
- (23) Chang, E.; Thekkekk, N.; Yu, W. W.; Colvin, V. L.; Drezek, R. Evaluation of quantum dot cytotoxicity based on intracellular uptake. *Small* **2006**, *2*, 1412–1417.
- (24) Hoshino, A.; Fujioka, K.; Oku, T.; Suga, M.; Sasaki, Y. F.; Ohta, T.; Yasuhara, M.; Suzuki, K.; Yamamoto, K. Physicochemical properties and cellular toxicity of nanocrystal quantum dots depend on their surface modification. *Nano Lett.* **2004**, *4*, 2163–2169.
- (25) Rzigalinski, B. A.; Strobl, J. S. Cadmium-containing nanoparticles: Perspectives on pharmacology and toxicology of quantum dots. *Toxicol. Appl. Pharmacol.* **2009**, *238*, 280–288.
- (26) Kirchner, C.; Liedl, T.; Kuder, S.; Pellegrino, T.; Munoz Javier, A.; Gaub, H. E.; Stolzle, S.; Fertig, N.; Parak, W. J. Cytotoxicity of colloidal CdSe and CdSe/ZnS nanoparticles. *Nano Lett.* **2005**, *5*, 331–338.



- (27) Priester, J. H.; Stoimenov, P. K.; Mielke, R. E.; Webb, S. M.; Ehrhardt, C.; Zhang, J. P.; Stucky, G. D.; Holden, P. A. Effects of soluble cadmium salts versus CdSe quantum dots on the growth of planktonic *Pseudomonas aeruginosa*. *Environ. Sci. Technol.* **2009**, *43*, 2589–2594.
- (28) Geys, J.; Nemmar, A.; Verbeken, E.; Smolders, E.; Ratoi, M.; Hoylaerts, M. F.; Nemery, B.; Hoet, P. H. M. Acute toxicity and prothrombotic effects of quantum dots: Impact of surface charge. *Environ. Health Perspect.* **2008**, *116*, 1607–1613.
- (29) Ryman-Rasmussen, J. P.; Riviere, J. E.; Monteiro-Riviere, N. A. Surface coatings determine cytotoxicity and irritation potential of quantum dot nanoparticles in epidermal keratinocytes. *J. Invest. Dermatol.* **2007**, *127*, 143–153.
- (30) Mahendra, S.; Zhu, H.; Colvin, V. L.; Alvarez, P. J. Quantum dot weathering results in microbial toxicity. *Environ. Sci. Technol.* **2008**, *42*, 9424–9430.
- (31) Bouldin, J. L.; Ingle, T. M.; Sengupta, A.; Alexander, R.; Hannigan, R. E.; Buchanan, R. A. Aqueous toxicity and food chain transfer of quantum dots in freshwater algae and *Ceriodaphnia dubia*. *Environ. Toxicol. Chem.* **2008**, *27*, 1958–1963.
- (32) Slaveykova, V. I.; Startchev, K.; Roberts, J. Amine- and carboxyl-quantum dots affect membrane integrity of bacterium *Cupriavidus metallidurans* CH34. *Environ. Sci. Technol.* **2009**, *43*, 5117–5122.
- (33) Li, Y.-Q.; Wang, H.-Q.; Wang, J.-H.; Guan, L.-Y.; Liu, B.-F.; Zhao, Y.-D.; Chen, H. A highly efficient capillary electrophoresis-based method for size determination of water-soluble CdSe/ZnS core-shell quantum dots. *Anal. Chim. Acta* **2009**, *647*, 219–225.
- (34) Pereira, M.; Lai, E. P. C.; Hollebone, B. Characterization of quantum dots using capillary zone electrophoresis. *Electrophoresis* **2007**, *28*, 2874–2881.
- (35) Song, X.; Li, L.; Qian, H.; Fang, N.; Ren, J. Highly efficient size separation of CdTe quantum dots by capillary gel electrophoresis using polymer solution as sieving medium. *Electrophoresis* **2006**, *27*, 1341–1346.
- (36) Vicente, G.; Colon, L. A. Separation of bioconjugated quantum dots using capillary electrophoresis. *Anal. Chem.* **2008**, *80*, 1988–1994.
- (37) Zhang, Y.-H.; Zhang, H.-S.; Ma, M.; Guo, X.-F.; Wang, H. The influence of ligands on the preparation and optical properties of water-soluble CdTe quantum dots. *Appl. Surf. Sci.* **2009**, *255*, 4747–4753.
- (38) Pereira, M.; Lai, E. P. C. Capillary electrophoresis for the characterization of quantum dots after non-selective or selective bioconjugation with antibodies for immunoassay. *J. Nanobiotechnol.* **2008**, *6*, 1–15.
- (39) Shao, L. W.; Dong, C. Q.; Huang, X. Y.; Ren, J. C. Using capillary electrophoresis mobility shift assay to study the interaction of CdTe quantum dots with bovine serum albumin. *Chin. Chem. Lett.* **2008**, *19*, 707–710.
- (40) Rundlett, K. L.; Armstrong, D. W. Methods for the estimation of binding constants by capillary electrophoresis. *Electrophoresis* **1997**, *18*, 2194–2202.
- (41) Her, N.; Amy, G.; Foss, D.; Cho, J. Variations of molecular weight estimation by HP-size exclusion chromatography with UVA versus online DOC detection. *Environ. Sci. Technol.* **2002**, *36*, 3393–3399.
- (42) Zhao, S.; Chen, X.; Hu, Z. Determination of hesperidin and naringin by micellar electrokinetic chromatography using a new recording mode. *Chromatographia* **2003**, *57*, 593–598.
- (43) Dunkellog, R.; Rüttinger, H. H.; Peisker, K. Comparative study for the separation of aquatic humic substances by electrophoresis. *J. Chromatogr., A* **1997**, *777*, 355–362.
- (44) Schmitt-Kopplin, P.; Garrison, A. W.; Perdue, E. M.; Freitag, D.; Kettrup, A. Capillary electrophoresis in the analysis of humic substances. Facts and artifacts. *J. Chromatogr., A* **1998**, *807*, 101–109.
- (45) Kawaoka, J.; Gomez, F. A. Use of mobility ratios to estimate binding constants of ligands to proteins in affinity capillary electrophoresis. *J. Chromatogr., B: Anal. Technol. Biomed. Life Sci.* **1998**, *715*, 203–210.
- (46) Yang, J.; Bose, S.; Hage, D. S. Improved reproducibility in capillary electrophoresis through the use of mobility and migration time ratios. *J. Chromatogr., A* **1996**, *735*, 209–220.
- (47) Lead, J. R.; Wilkinson, K. J.; Starchev, K.; Canonica, S.; Buffle, J. Determination of diffusion coefficients of humic substances by fluorescence correlation spectroscopy: Role of solution conditions. *Environ. Sci. Technol.* **2000**, *34*, 1365–1369.
- (48) Slaveykova, V. I.; Startchev, K. Effect of natural organic matter and green microalgae on carboxyl-polyethylene glycol coated CdSe/ZnS quantum dots stability and transformations under freshwater conditions. *Environ. Pollut.* **2009**, *157*, 3445–3450.
- (49) Pyell, U. CE characterization of semiconductor nanocrystals encapsulated with amorphous silicon dioxide. *Electrophoresis* **2008**, *29*, 576–589.
- (50) Navarro, D. A.; Banerjee, S.; Aga, D. S.; Watson, D. F. Partitioning of hydrophobic CdSe quantum dots into aqueous dispersions of humic substances: Influence of capping-group functionality on the phase-transfer mechanism. *J. Colloid Interface Sci.* **2010**, *348*, 119–128.
- (51) Dong, C.; Qian, H.; Fang, N.; Ren, J. Study of fluorescence quenching and dialysis process of CdTe quantum dots, using ensemble techniques and fluorescence correlation spectroscopy. *J. Phys. Chem. B* **2006**, *110*, 11069–11075.
- (52) Mancini, M. C.; Kairdolf, B. A.; Smith, A. M.; Nie, S. Oxidative quenching and degradation of polymer-encapsulated quantum dots: New insights into the long-term fate and toxicity of nanocrystals in vivo. *J. Am. Chem. Soc.* **2008**, *130*, 10836–10837.
- (53) Blaudeck, T.; Zenkevich, E. I.; Cichos, F.; von Borczyskowski, C. Probing wave functions at semiconductor quantum-dot surfaces by non-FRET photoluminescence quenching. *J. Phys. Chem. C* **2008**, *112*, 20251–20257.
- (54) Durisic, N.; Wiseman, P. W.; Grütter, P.; Heyes, C. D. A common mechanism underlies the dark fraction formation and fluorescence blinking of quantum dots. *ACS Nano* **2009**, *3*, 1167–1175.
- (55) Fetsch, D.; Fetsch, M.; Pena Mendez, E. M.; Havel, J. Humic acid capillary zone electrophoresis adsorption on capillary walls, separation in metal ion supplemented buffer and the fingerprints. *Electrophoresis* **1998**, *19*, 2465–2473.
- (56) Engebretson, R. R.; Amos, T.; von Wandruszka, R. Quantitative approach to humic acid associations. *Environ. Sci. Technol.* **1996**, *30*, 990–7.
- (57) Hosse, M.; Wilkinson, K. J. Determination of electrophoretic mobilities and hydrodynamic radii of three humic substances as a function of pH and ionic strength. *Environ. Sci. Technol.* **2001**, *35*, 4301–4306.
- (58) Ohshima, H. Approximate analytic expression for the electrophoretic mobility of a spherical colloidal particle. *J. Colloid Interface Sci.* **2001**, *239*, 587–590.
- (59) Stewart, D. T. R.; Celiz, M. D.; Vicente, G.; Colón, L. A.; Aga, D. S. Potential use of capillary zone electrophoresis in size characterization of quantum dots for environmental studies. *TrAC, Trends Anal. Chem.* **2011**, *30*, 113–122.